Asian Journal of Medical Sciences 4(2): 66-74, 2012
ISSN: 2040-8773

Submitted: February 16, 2012 Accepted: March 24, 2012 Published: April 30, 2012

Variational Level Set Segmentation and Bias Correction of Fused Medical Images

[1]M. Renugadevi, [1]Deepa Varghese, [1]V. Vaithiyanathan and [2]N. Raju
[1]School of Computing,
[2]School of EEE, SASTRA University, Thanjavur, India

Abstract: Medical image fusion and segmentation has high impact on the digital image processing due to its spatial resolution enhancement and image sharpening. It has been used to derive useful information from the medical image data that provides the most accurate and robust method for diagnosis. This process is a compelling challenge due to the presence of inhomogeneities in the intensity of images. For addressing this challenge, the region based level set method is used for segmenting the fused medical images with intensity inhomogeneity. First, the IHS-PCA based fusion method is employed to fuse the images with intensity inhomogeneity which is then filtered using the homomorphic filter. Then based on the model of the fused image and the derived local intensity clustering property, the level set energy function is defined. This function is minimized to simultaneously partition the image domain and to estimate the bias field for the intensity inhomogeneity correction. The outstanding performance of this approach is illustrated using images of various modalities. Experimental results highlight the effectiveness and advantage of this approach with the help of various metrics and the results are found to be good and accurate.

Key words: Bias field, IHS (Intensity Hue Saturation), image fusion, intensity inhomogeneity, PCA (Principal Component Analysis), segmentation

INTRODUCTION

Medical imaging helps the global healthcare system for non-invasive diagnose, treatment and cure. The current research on medical image analysis mainly focus on image fusion and segmentation as it is an effective means of mapping the anatomy of the subject. Fused medical images integrates multimodal medical image to single image with vivid and accurate description of the same object. As they endow with both anatomical and functional information, it assists in scheduling surgical procedures. Some of the image modalities are Magnetic Resonance Imaging (MRI), Computed Tomography (CT), Positron Emission Tomography (PET) and Single-Photon Emission Computerized Tomography (SPECT) that provides quantification of tissue volumes, diagnosis, study of anatomical structure and treatment planning. MRI images provide detailed information on soft tissue with more distortion and do not use ionizing radiation. ACT scan combines many X-ray images taken from different angles and provides high resolution information on bone structure tissue with less distortion. For PET and SPECT scan, a radioactive substance known as tracer is used, which reveals the working of organs and tissues and the blood flow to and from organs. The difference in SPECT and PET scan is that the former emit gamma rays of varying energies and is used for estimating the relative myocardial blood flow but is affected by attenuation artifacts, while the latter emits positron which are more stable. SPECT measures the concentration of chemicals injected into the body and thus gives images of the chemical function of body parts. The fusing of MRI and CT image helps a physician to obtain a better visualization of the patient's condition as it clearly identifies both the bone structure and tissue structure in a single image. MRI image has high spatial resolution and shows the tissue anatomy but PET images are low resolution images but can convey the function of the organ. So the fusion of MRI and PET enhance the spatial resolution of the functional images without spatial distortion. SPECT/MRI fusion like all other fusion is widely used as it helps for accurate diagnosis.

Image segmentation is another important area in the medical image guide surgery. It provides richer information in numerous biomedical imaging applications and for the delineation of anatomical structures. It is defined as the process of partitioning the given image into interested domains with least human manipulation. Active contour model which is based on the theory of surface evolution and geometric flows have been the successful one among the several segmentation methods (Kass *et al*., 1988; Blake and Isard, 1998; Paragios and Deriche, 2000). The two main categories of the existing active contour models are Edge based models (Xu and Prince, 1998; Caselles *et al*., 1993; Kichenassamy *et al*., 1996) and Region based models (Ronfard, 1994; Mumford and

Corresponding Author: M. Renugadevi, School of Computing, SASTRA University, Thanjavur, India

Shah, 1989; Chan and Vese 2001; Paragios and Deriche, 2002, Caselles *et al*., 1997; Tsai *et al*., 2001; Chunming *et al*., 2007; Zhang *et al*., 2010). Edge based active contour model use the local edge detector information that depends on the image gradient to evolve the contour toward the object boundaries. Region based active contour model use the statistical information to build the region descriptor to guide the motion of the contour. The latter model has better performance over the former since it is able to segment the objects with weak boundaries and less sensitive to the initial contour position. One of the most popular methods in the region based image segmentation is the level set method (Sethian, 1999) which is a numerical technique for capturing dynamic interfaces and shapes. It has been introduced by Osher and Sethian (1988) and most widely used because of their advantageous properties such as topology adaptability and robustness to initialization.

Nowadays, level set method turns its sight to deal with intensity inhomogeneous images. It often exists in the real medical images due to imperfection in the imaging device and susceptibility effect induced by the object being imaged. Particularly in MRI images, non uniform magnetic fields produced by radio-frequency coils as well as from variations in object susceptibility causes intensity inhomogeneity. The information from the magnetic resonance images can be added to the CT or PET or SPECT image that would help surgeons for better diagnostics. If intensity inhomogeneous MRI image is fused with another image then the resultant image may not serve the purpose of fusion. Segmentation of such fused images usually requires intensity inhomogeneity correction. Recently, (Chunming *et al*., 2011) proposed a Local Clustering based Variational Level Set (LCVLS) model for simultaneous segmentation and bias correction. Our idea is to use this model to segment the fused image and also for bias correction.

In this study, a novel approach for segmenting and bias correcting the fused medical image is presented using the level set method. For this process, initially the low resolution medical image (CT, PET and SPECT) and the Intensity Inhomogeneous Magnetic Resonance Imaging (IIH_MRI) image are selected. The selected images (CT/MRI, PET/MRI and SPECT/MRI) are fused using IHS-PCA fusion method (Changtao *et al*., 2010) to get the combined information in a single image. Then the segmentation and the intensity inhomogeneity correction (bias correction) is done by employing the Local Clustering based Variational Level Set (LCVLS) model (Chunming *et al*., 2011).

Related works: The objective of the image fusion is to reduce the ambiguity, minimize redundancy in the fused image and to achieve optimal resolution in the spatial and spectral domains. Several methods are there to modulate lower resolution images such as the IHS, PCA and DWT. Changtao *et al*. (2010) has proposed of MRI/PET fusion based on the combination of IHS and PCA where Daneshvar (Sabalan and Hassan, 2007) speaks about the same fusion with human retina model. The wavelet transformation is used to fuse medical images in Zhang *et al*. (2008) and Jionghua *et al*. (2010). As we are not concentrating specifically on any two images for fusion we have chosen the conventional fusion method based on IHS as it is well suited for practical applications. A modified fusion based on IHS for three bands and four bands are described in Choi (2006) and are termed as Fast IHS (FIHS) and Generalized IHS (GIHS) respectively to reduce the spectral distortion. However, FIHS performs better than IHS, it also results in slight distortion. So the new Spectral Adjusted IHS (SAIHS) method is proposed in to remove the distortion efficiently. Even the method is based on the spectral characteristics of the sensors for satellite images, it is showing good results for medical images.

Region based models aim to partition the image into regions by utilizing the statistical image information. It builds the region descriptor that guides the motion of the active contour model. Initially, the region based active contour model that works well for the images with two regions was proposed by Chan and Vese (2001). They extended their work in Vese and Chan (2002) and proposed Piecewise Constant (PC) model based on the Mumford-Shah segmentation in which multiple level set functions are used to represent the multiple regions. However, it is not suitable for the images with intensity inhomogeneities.

In order to segment the images with intensity inhomogeneities, the Piecewise Smooth (PS) model is proposed (Vese and Chan, 2002; Tsai *et al*., 2001). But these models are computationally inefficient and expensive. In Chunming *et al*. (2007) Li proposed the Local Binary Fitting (LBF) method which utilizes the local image information and therefore it is able to segment the objects with intensity inhomogeneities. It performs well than the PC and PS models. Zhang *et al*. (2010) proposed the new region based active contour model by introducing the Local Image Fitting (LIF) energy to extract local image information which can be used to segment the intensity inhomogeneous images. This method has less computational complexity than the LBF method. The Region Scalable Fitting (RSF) Energy method was proposed by Chuming *et al*. (2011) which performs well for the images with weak object boundaries. It is also the efficient method to segment the medical images with intensity inhomogeneities (Chunming *et al*., 2008). However, these methods are quite sensitive to the initialization of the contour for the level set evolution and also not suitable for the intensity inhomogeneous correction.

Chunming *et al*. (2011) proposed a local clustering based variational level set framework for simultaneous intensity inhomogeneous image segmentation and bias correction. First, the local intensity clustering property is derived based on the model of the images with the intensity inhomogeneity. For the image intensities in the

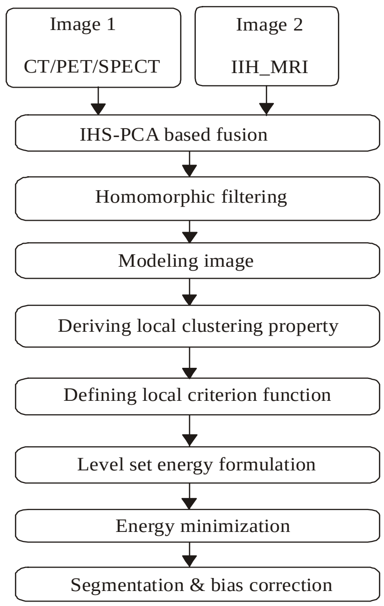

Fig. 1: Block diagram for the proposed method

neighbourhood of each point, the local intensity criterion function is defined which is then integrated with respect to the neighbourhood center to give a global criterion of image segmentation. In the level set formulation, to represent the partition of the image domain into distinct regions and a bias field, this criterion function defines energy in terms of the level set functions. Then the energy minimization is performed in the level set process to segment the images and also to estimate the bias field for the intensity inhomogeneity correction or bias correction.

PROPOSED METHODOLOGY

The proposed simultaneous level set segmentation and bias correction for the IHS-PCA fused medical image using the LCVLS model is explained in this section. Figure 1 shows the block diagram for the entire process.

Fusing and filtering: The fusion algorithm of the medical images is based on combination of IHS and PCA (Changtao *et al*., 2010; El-Mezouar *et al*., 2011). In IHS model we have to convert the red, green and blue components of the low resolution image to Intensity (I), Hue (H) and Saturation (S). The main conversion system methods are the linear, the triangular spectral mode and here the second method is followed and it results in a fused and enhanced spectral image. The input images can be any of the three categories. They are:

- IIH_MRI and CT
- IIH_MRI and PET
- IIH_MRI and SPECT

The low resolution image is transformed to IHS triangular model components. Normally in triangular spectral mode, the Intensity (I) which displays the brightness in a spectrum is calculated by:

$$I = R + G + B/3 \tag{1}$$

But if the intensity factor is near to high resolution image then the spectral resolution can be reduced. So that the spectral responses (El-Mezouar *et al*., 2011) of the sensors is used and the two constants a = 0.75 and b = 0.25 and an NIR band is introduced as it is used in satellite images. So Eq. (1) is replaced by:

$$I = R + a * G + b * B + NIR/3 \tag{2}$$

The property of spectral wavelength and the purity of the spectrum are Hue (H) and Saturation (S) respectively, and it can be expressed as:

$$H = G - B/3I - 3B,\ S = I - B/I \text{ if } B < R, G \tag{3}$$

$$H = B - R/3I - 3R + 1,\ S = I - R/I \text{ if } R < B, G \tag{4}$$

$$H = R - G/3I - 3G + 2,\ S = I - G/I, \text{ if } G < R, B \tag{5}$$

The corresponding inverse IHS transform as follows:

$$R = I(1 + 2S - 3SH),\ G = I(1 - S + 3SH),\ B = I(1 - S) \text{ if } B < R,G \tag{6}$$

$$R = I(1 - S),\ G = I(1 + 5S - 3SH),\ B = I(1 - 4S + 3SH), \text{ if } R < B, G \tag{7}$$

$$R = I(1 - 7S + 3SH),\ G = I(1 - S),\ B = I(1+8S - 3SH), \text{ if } G < R, B \tag{8}$$

After the conversion of RGB to IHS, histogram matching of the high resolution image and the intensity component of low resolution image is performed. The histogram matched high resolution image is termed as New Pan. The intensity component and New Pan is taken as principle component for PCA method. The weighted coefficients after PCA transform is done by calculating the Spatial Frequency (SF) of the original low resolution image (Yesou *et al*., 1993; Ehlers, 1991) and the old Pan. The relevance of SF is to measure the image blocks (Shutao *et al*., 2001; Eskicioglu and Fisher, 1995) calculated for image $f(x, y)$ with K × L pixels and is defined as:

$$SF = \sqrt{(RF)^2 + (CF)^2} \tag{9}$$

where, RF and CF are the row and column frequency, respectively.

$$RF = \sqrt{\frac{1}{KxL}\sum_{x=1}^{K}\sum_{y=2}^{L}\left[f(x,y) - f(x,y-1)\right]^2}$$

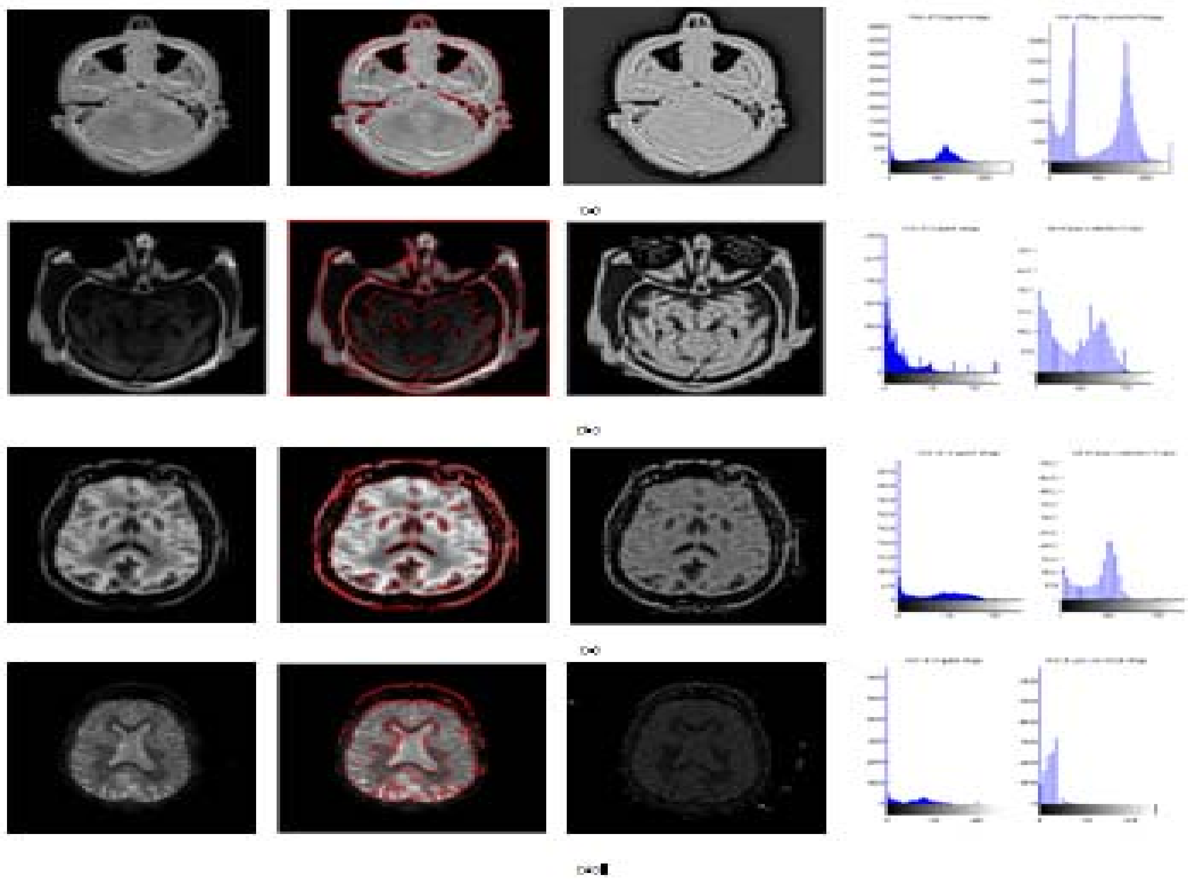

Fig. 2: Segmentation and bias correction of fused images. CT/MRI fused image segmentation and bias correction is shown (a) and (b). PET/MRI and SPECT/MRI fused image segmentation and bias correction is shown in (c) and (d), respectively. Column 1 shows the homomorphic filtered image. Column 2 shows the segmented result. Column 3 shows the bias corrected image. Histogram of fused image and bias corrected image is shown in column 4 and 5

$$CF = \sqrt{\frac{1}{KxL}\sum_{Y=1}^{L}\sum_{X=2}^{K}\left[f(x,y) - f(x-1,y)\right]^2} \quad (10)$$

The selection of two principal component weighted coefficients is shown with:

$$I = \alpha I_1 + \beta I_2 \quad (11)$$

where, I_1 and I_2 represent the two principal components after PCA. α and β are normalized SF values. The last step is to find the inverse of IHS transform of the new intensity, the old hue and saturation components which will results in the fused image.

Then the homomorphic filter is applied to the fused image prior to the segmentation process. Generally, homomorphic filter is a non-linear filtering technique for enhancing an image by increasing the contrast and by normalizing the brightness across the image at the same time. It is performed with Butterworth low pass filter which is defined as:

$$H(u, v) = 1/1+[D(u, v)/D_0]^{2n}$$

where, n denotes the order of filter, D_0 is the cutoff distance from center and D(u,v) is given as:

$$D(u, v) = [(u - M/2)^2 + (v - M/2)^2]^{1/2}$$

where, m and n denotes the number of rows and columns of the fused image. The filtered output is shown in Fig. 2.

LCVLS model: Let an image I is considered as a function I : $I:\Omega \to \Re$ defined on a continuous domain. And to deal with intensity inhomogeneities, it is modeled as:

$$I = bJ + n \quad (12)$$

where, J is the true image which is assumed to be piecewise constant since it measures an intrinsic physical property of the objects, b is a bias field component that denotes the intensity inhomogeneity and assumed to be varying slowly and n is additive noise that is assumed to be zero-mean Gaussian noise. Based on this model and assumptions, the criteria is defined as an energy functional in terms of the regions Ω_i, the constants c_i, and the bias field b and is minimized to get the optimal regions $\{\hat{\Omega}_i\}_{i=1}^N$, constants $\{\hat{c}_i\}_{i=1}^N$ and the bias field $\hat{b}$ that results in the image segmentation and bias field estimation.

However due to the presence of intensity inhomogeneities, it is difficult to segment the regions based on the pixel intensities. Therefore a useful property of local intensities is derived which is referred as a local intensity clustering property. To derive this, a circular neighborhood with a radius ρ centered at each point $y \in \Omega$ is defined by:

$$O_y \triangleq \{x : |x - y| \le \rho\}$$

The partition of the neighborhood O_y is induced by the partition $\{\Omega_i\}_{i=1}^N$ of the entire domain Ω. This property allows applying the K-means clustering to classify the intensities in the neighborhood O_y into N clusters, with centers $m_i \approx b(y)\, c_i$, i = 1, 2, …, N. Then specifically for classifying the intensities I(x) in the neighborhood O_y, a clustering criterion is defined as:

$$\varepsilon_y = \sum_{i=1}^{N} \int_{\Omega_i} K(y - x)\left|I(x) - b(y)c_i\right|^2 dx \qquad (13)$$

where, K(y-x) is kernel function (nonnegative window function), such that K(y-x) = 0 for $x \notin O_y$. Equation (13) is called local clustering criterion function that evaluates the classification of the intensities in the neighborhood O_y. The smaller value of ε_y yields the better classification. So to minimize the ε_y with respect to y over the image domain Ω, an energy is defined as:

$$\varepsilon \triangleq \int \left(\sum_{i=1}^{N} \int_{\Omega_i} K(y - x)\left|I(x) - b(y)c_i\right|^2 dx \right) dy \qquad (14)$$

Here the kernel function K is truncated Gaussian function defined by:

$$K(u) = \begin{cases} \dfrac{1}{a} e^{-|u|^2/2\sigma^2}, & for\ |u| \le \rho \\ 0, & otherwise \end{cases} \qquad (15)$$

where, a is a normalization constant such that $\int K(u) = 1$, σ is the scale parameter of the Gaussian function and ρ is the radius of the neighborhood O_y.

The above defined energy functional is in terms of the regions $\Omega_1, \ldots, \Omega_N$. To derive the solution for the energy minimization problem, the energy is converted to a level set formulation. It can be done by representing the disjoint regions Ω_1, ..., Ω_N with number level set functions each with a regularization term. Generally, the level set function can take positive or negative signs to represent a partition of the domain Ω into disjoint regions Ω_1 and Ω_2.

Let $\phi : \Omega \to \Re$ be a level set function with two disjoint regions:

$$\Omega_1 = \{x : \phi(x) > 0\} \text{ and } \Omega_2 = \{x : \phi(x) < 0\} \qquad (16)$$

that forms a partition of the domain Ω. The level set formulation of the energy with N = 2 and N>2, called two phase and multiphase formulation, respectively. Here only the two phase formulation is considered.

In the two case level set formulation, the regions Ω_1 and Ω_2 can be represented with their membership function defined by $M_1(\phi) = H(\phi)$ and $M_2(\phi) = 1 - H(\phi)$ respectively, where H is the Heaviside function (Chunming *et al*., 2011). Thus, the energy functional can be expressed as:

$$\varepsilon = \int \sum_{i=1}^{N} \left(\int K(y - x)\left|I(x - b(y)ci\right| dy \right)^2 M_i(\phi(x))dx \qquad (17)$$

For convenience, the constants c_1, …, c_N can be represented as a vector $c = (c_1, \ldots, c_N)$. Thus the variables of the energy functional ε are the level set function ϕ, the vector c and the bias field b. So the energy functional ε can be written as:

$$\varepsilon(\phi, c, b) = \int \sum_{i=1}^{N} e_i(x) M_i(\phi(x))dx \qquad (18)$$

where, e_i function is defined by:

$$e_i(x) = \int K(y - x)\left|I(x) - b(y)c_i\right|^2 dy \qquad (19)$$

The variational level set formulation uses the above defined energy as the data term which is defined by:

$$F(\phi, c, b) = \varepsilon(\phi, c, b) + vL(\phi) + \mu \Re_p(\phi) \qquad (20)$$

where, $L(\phi)$ and $\Re_p(\phi)$ are the regularization terms defined below. The term $L(\phi)$ that computes the arc length of the zero level contour of ϕ is defined by:

$$L(\phi) = \int \left|\nabla H(\phi)\right| dx \qquad (21)$$

The term $\Re_p(\phi)$ is defined by:

$$\Re_p(\phi) = \int p(\left|\nabla \phi\right|)dx \qquad (22)$$

where, p is a potential or energy density function $p:[0, \infty) \to \Re$ such that $p(s) = (1/2)(s - 1)^2$. With this potential

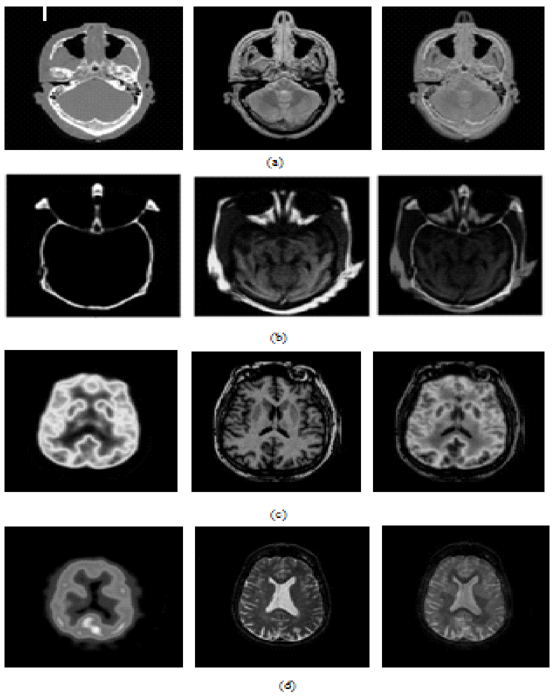

Fig. 3: IHS-PCA based fusion process. (a) and (b) showsCT/MRI fusion, (c) shows PET/MRI fusion and (d) shows SPECT/MRI fusion. Column 1 and 2 shows original images and column 3 shows respective fused image

p, the energy term $U_p(\mathbf{N})$ in (20) is minimized by maintaining |v **N**| 1 which is called signed distance property. And so $U_p(\mathbf{N})$ is called distance regularization term (Chunming *et al*., 2010).

The energy F(**N**, c, b) is minimized by an iteration process with respect to each of its variables (Chunming *et al*., 2011). Thus solution for the energy minimization problem is achieved by minimizing this energy term that results in the image segmentation given by the level set function **N** and estimation of the bias field b.

EXPERIMENTAL RESULTS

In order to validate the theoretical analysis, efforts were taken for quantitative analysis. In each step of experimentation, the quantitative metrics are taken depending on the base of results. The experiment is conducted on the selected medical images with 256×256 dimensions. Initially the intensity inhomogeneous MRI images are selected to get individually fused with CT, PET and SPECT images. Figure 3 shows the IHS-PCA based fusion process for the four different pairs of images. For evaluating spatial and spectral quality of fused medical images, metrics such as relative bias, relative variance, Correlation Coefficient (CC), Universal Image Quality Index (UIQI), are taken. Bias is the difference between the mean value of input and output images and relative bias is the ratio between the bias and the mean value of the original image. The relative variance is calculated by dividing the variance difference of the original and the fused image by the variance of the original low resolution image.

Table 1: Objective indicators for IHS-PCA based medical image fusion

Parameters	Fuse 1	Fuse 2	Fuse 3	Fuse 4
Relative Bias	0.122797	0.5052573	0.182485	0.071502
Relative Variwxe	0.006214	0.575788	0.062028	0.005282
CC	0.95781	0.870488	0.856781	0.929975
UIQI	0.991473	0.899124	0.985668	0.997616

Correlation Coefficient (CC) is the most widely used similarity metric which indicates the likeness between the original low resolution medical image and the fused image. With x and y as original and fused image and $\bar{x}$ and $\bar{y}$ as their mean value, the CC for MxN image is calculated by:

$$CC(x/y) = \frac{\sum_{i=1}^{M}\sum_{j=1}^{N}\left(x_{i,j}-\bar{x}\right)\left(y_{i,j}-\bar{y}\right)}{\sqrt{\sum_{i=1}^{M}\sum_{j=1}^{N}\left(x_{i,j}-\bar{x}\right)^2\sum_{i=1}^{M}\sum_{j=1}^{N}\left(y_{i,j}-\bar{y}\right)^2}} \quad (23)$$

UIQI:

The Universal Image Quality Index (UIQI) (Wang and Bovik, 2002) range from -1 to +1. It is calculated by considering the information contained in reference image such as loss of correlation, luminance distortion and contrast distortion. The performance evaluation for each fused image is shown in Table 1:

$$UIQI = \frac{\sigma_{AB}}{\sigma_A\sigma_B}\cdot\frac{2\mu_A\mu_B}{\mu^2{}_A+\mu^2{}_B}\cdot\frac{2\sigma_A\sigma_B}{\sigma^2{}_A+\sigma^2{}_B} \quad (24)$$

where, **F** represents the standard deviation and **:** represents the mean value. The first term in Eq. (24) is the correlation coefficient, the second term represents the mean luminance and the third measures the contrast distortion UIQI is also used to similarity between the two images.

Then the fused image is employed with the homomorphic filter to make the images suitable for the segmentation and bias correction. The output of the LCVLS model is shown in Fig. 2. This figure shows the segmented and bias corrected images along with the filtered images. The histogram of the filtered image and the bias corrected image is also shown in Fig. 2 which depicts that intensity inhomogeneity of the fused image is removed more efficiently using the proposed approach. Also the performance of the segmentation process is evaluated using statistical measures such as Rand Index (RI), Global Consistency Error (GCE) and Variation of Information (VI).

The resemblance between two data clusters can be measured using rand index (Unnikrishnan *et al*., 2007). With a given set of n elements, two segments of S and two sets X and Y, Rand index (R) can be defined as:

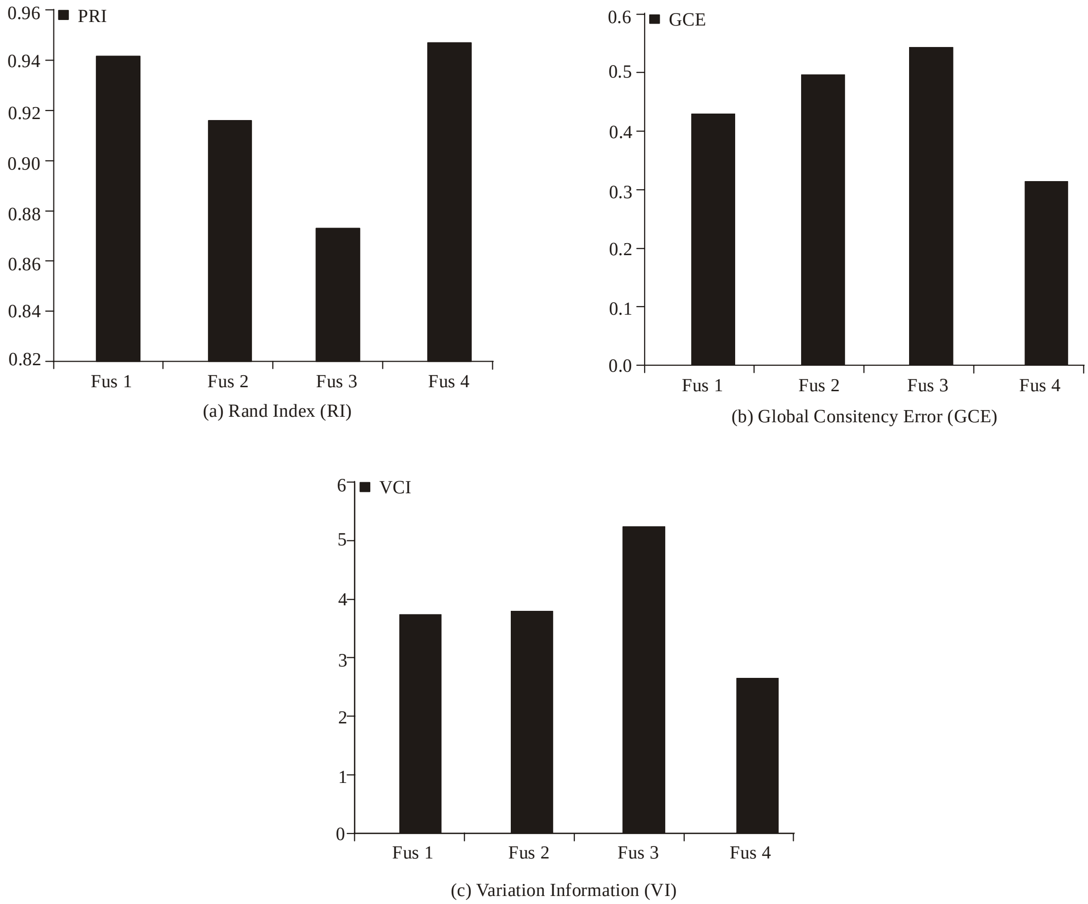

Fig. 4: Statiscal measure for segmentation of four fused images

Table 2 : Performance measure for the segmentation results of fused images

Fused Image	RI	GCE	VI
CT/MRI	0.942	0.4391	3.7868
CT/MRI	0.9188	0.5051	3.9108
PET/MRI	0.8736	0.5561	5.2376
SPECT/MRI	0.9484	0.3217	2.6655

$$R = \frac{a+b}{a+b+c+d} = \frac{a+b}{\binom{n}{2}} \qquad (25)$$

where, a + b represents the number of agreements among X and Y and c + d represents the number of disagreements among X and Y. The value of R falls in the range of 0 to 1 depends upon the similarities between the given clusters.

Global Consistency Error (GCE) is one of the objective evaluations which measures to quantify the consistency between the image segmentations (Unnikrishnan *et al*., 2007). It is defined as:

$$GCE(s_1, s_2) = \frac{1}{N}\min\left\{\sum E(s_1, s_2, p_i), \sum E(s_2, s_1, p_i),\right\} \qquad (26)$$

where, $s_1$and s_2 are two segments that contain the given point p_i. It gives the error values in [0, 1] in which lower value signifies the better segmentation.

Variation of Information (VI) is a quality measure used to define the distance between two segmentations (Unnikrishnan *et al*., 2007). If X and Y are the two clustering where $X = \{X_1, X_{2,\dots,} X_K\}, p_i = |X_i|/n, n = \sum_k |X_i|$ then variation of information is defined as:

$$VI(X, Y) = H(X) + H(Y) - 2I(X, Y) \qquad (27)$$

where H(X) and H(Y) are entropy of X and Y respectively and 2I(X, Y) is mutual information between X and Y. The lower VI value indicates the greater similarity. These objective evaluations are performed in the segmented outputs and the results are shown in Table 2. Figure 4 shows the graphical representation of the statistical measures of segmentation. The higher values of RI and lower values of GCE and VI indicate the better segmentation.

CONCLUSION

This study presents the novel approach for segmenting and correcting the intensity inhomogeneity in the IHS-PCA fused medical images using the LCVLS model. This model efficiently utilizes the local image information and therefore able to simultaneously segment and bias correct the images with intensity inhomogeneity. It has desirable performance for segmenting and bias correcting the medical images of various modalities. It is more robust to initialization and good approximation to the bias field. In addition, the subjective and objective evaluation of this approach proves to be effective and efficient in the process of medical image fusion, segmentation and bias correction. With this appreciable performance, we expect that the proposed approach will find its utility in the area of medical diagnosis.

ACKNOWLEDGMENT

Authors wish to thank Dr. N. Sairam and Dr. B. Shanthi, Professors of CSE Department, SASTRA University for their time & technical support. Also we wish to thank Prof. E. Koperundevi of English Department, SASTRA University for her linguistic support.

REFERENCES

Blake and M. Isard, 1998. Active Contours. MA: Springer, Cambridge.

Caselles, V., F. Catte, T. Coli and F. Dibos, 1993. A geometric model for active contours in image processing. Numer. Math., 66(1): 1-31.

Caselles, V., R. Kimmel and G. Sapiro, 1997. Geodesic active contour. Int. Comput. Vis., 22(1): 61-79.

Chan, T. and L. Vese, 2001. Active contours without edges. IEEE T. Image Process., 10(2): 266-277.

Changtao, H., L. Quanxi, L. Hongliang and W. Haixu, 2010. Multimodal medical image fusion based on IHS and PCA: Symposium on security detection and information processing. Procedia Eng., 7: 280-285.

Choi, M., 2006. A new intensity-hue-saturation fusion approach to image fusion with a tradeoff parameter. IEEE T. Geosci. Remote, 44(6): 1672-1682.

Chunming, L., C. Kao, J. Gore and Z. Ding, 2007. Implicit Active Contours Driven by Local Binary Fitting Energy. IEEE Conference on Computer Vision and Pattern Recognition.

Chunming, L., C. Kao, J. Gore and Z. Ding, 2008. Minimization of region-scalable fitting energy for image segmentation. IEEE T. Image Process., 17(10): 1940-1949.

Chunming, L., C. Xu, C. Gui and M.D. Fox, 2010. Distance regularized level set evolution and its application to image segmentation. IEEE T. Image Process., 19(12): 3243-3254.

Chunming, L., R. Huang, Z. Ding, C. Gatenby, D.N. Metaxas and J.C. Gore, 2011. A level set method for image segmentation in the presence of intensity inhomogeneities with application to MRI. IEEE T. Image Process., 20(7): 2007-2016.

Ehlers, M., 1991. Multisensory image fusion techniques in remote sensing. ISPRS J. Photogramm., 46: 19-30.

Eskicioglu, A.M. and P.S. Fisher, 1995. Image quality measures and their performance. IEEE T. Commun., 43(12): 2959-2965.

Jionghua, T., W. Xue, Z. Jingzhou and W. Suhuan, 2010. Wavelet-based Texture Fusion of CT/MRI Images. International Congress on Image and Signal Processing.

Kass, M., A. Witkin and D. Terzopoulos, 1988. Snakes: Active contour models. Int. J. Comput. Vis., 1(4): 321-331.

Kichenassamy, S., A. Kumar, P. Olver, A. Tannenbaum and A.Y. Jr, 1996. Conformal curvature flows: From phase transitions to active vision. Arch. Ration. Mech. Anal., 134(3): 275-301.

El-Mezouar, M.C., T. Nasreddine, K. Kidiyo and R. Joseph, 2011. An IHS-based fusion for color distortion reduction and vegetation enhancement in IKONOS imagery. IEEE T. Geosci. Remote., 49(5): 1590-1602.

Mumford, D. and J. Shah, 1989. Optimal approximations by piecewise smooth functions and associated variational problems. Comrnun. Pure AppI. Math., 42(5): 577-685.

Osher, S. and J. Sethian, 1988. Fronts propagating with curvature-dependent speed: Algorithms based on Hamilton-Jacobi formulations. J. Comput. Phys., 79(1): 12-49.

Paragios, N. and R. Deriche, 2000. Geodesic active contours and level sets for the detection and tracking of moving objects. IEEE T. Pattern Anal. Mach. Intell., 22(3): 226-280.

Paragios, N. and R. Deriche, 2002. Geodesic active regions and level set methods for supervised texture segmentation. Int. J. Comput. Vis., 46(3): 223-247.

Ronfard, R., 1994. Region-based strategies for active contour models. Int. 1. +Comp. Vis., 13(2): 229-251.

Sabalan, D. and G. Hassan, 2007. MRI and PET images fusion based on human retina model. J. Zhejiang Univ-Sc A., 8(10): 1624-1632.

Sethian, J., 1999. Level Set Methods and Fast Marching Methods. 2nd Edn., Springer, New York.

Shutao, L., T.K. James and W. Yaonan, 2001. Combination of images with diverse focuses using the spatial frequency. Inform. Fusion, 2: 169-176.

Tsai, A., Yezzi and A.S. Willsky, 2001. Curve evolution implementation of the Mumford-Shah functional for image segmentation, denoising, interpolation and magnification. IEEE T. Image Process., 10(8): 1169-1186.

Unnikrishnan, R., C. Pantofaru and M. Hebert, 2007. Toward objective evaluation of image segmentation algorithms. IEEE T. Pattern Anal. Mach. Intell., 29(6): 929-944.

Vese, L. and T. Chan, 2002. A multiphase level set framework for image segmentation using the mumford and Shah model. Int. J. Compo Vis., 50(3): 271-293.

Wang, Z. and A.C. Bovik and 2002. A universal image quality index. IEEE Signal Process. Lett., 9(3): 81-84.

Xu, C. and Prince, 1998. Snakes, shapes and gradient vector flow. IEEE T. Image Process., 7(3): 359-369.

Yesou, H., Y. Besnus and Y. Rolet, 1993. Extraction of spectral information from Landsat TM data and merger with SPOT panchromatic imagery. ISPRS J. Photogramm., 48(5): 23-36.

Zhang, J.Z., T. Li and J. Wu, 2008. Research of medical image fusion based on wavelet transform. Chinese J. Biomed. Eng., 27: 521-525.

Zhang, K., H. Song and L. Zhang, 2010. Active contours driven by local image fitting energy. Pattern Recogn., 43(4): 1199-1206.